

## Temperature-Programmed Desorption on the Unstable Lattice Oxygen of Praseodymium Oxide

YOSHIO TAKASU,\* MASAKI MATSUI,\* HIROSHI TAMURA,\* SHIGEO KAWAMURA,\*  
YOSHIHARU MATSUDA,\* AND ISAMU TOYOSHIMA†

\* Faculty of Engineering, Yamaguchi University, Tokiwadai, Ube, Yamaguchi 755, Japan, and

† Research Institute for Catalysis, Hokkaido University, Sapporo 060, Japan

Received September 5, 1980; revised November 11, 1980

A TPD (temperature-programmed desorption) study on the unstable lattice oxygen from praseodymium oxide has been made with a view to know catalytic behaviors of such an unstable lattice oxygen to the oxidation reactions. Five different oxygen peaks [ $\alpha$  (340°C),  $\alpha'$  (380°C),  $\beta$  (400°C),  $\gamma$  (440°C), and  $\delta$  (500°C)] were observed on the TPD spectra from the oxide between 25 and 600°C, and the thermal behaviors of the  $\beta$ ,  $\gamma$ ,  $\delta$  peak oxygens were investigated as functions of oxygen absorption temperature, pressure, and time. The total amount of oxygen desorbed (evolved) between 25 and 600°C from  $\text{Pr}_6\text{O}_{11}$ , which is one of the oxides having a stable composition, corresponded to 7.5% of total oxygen in the oxide. The absorption rates of oxygens for each peaks were very fast, and the activation energies for desorption were rather high ranging from 34 to 43 kcal/mol. Among these three peaks, only the  $\beta$  peak oxygen reacted with nitric oxide at 300°C.

### INTRODUCTION

In recent years, many investigators have reported on the reactivity and behavior of lattice oxygen in metallic oxides to catalytic oxidation of olefines or the other oxidation reactions. The main interest in such study is whether the lattice oxygen shows better catalytic properties, activity or selectivity, compared to the adsorbed oxygen on the oxide. For example, Keulks (1) found on the oxidation of propylene over the bismuth-molybdate catalyst that the catalytic activity is directly related to the rate of diffusion of the oxygen ion through the lattice; however, Moro-oka and co-workers (2) have found no convincing evidence that the selectivity to the formation of acrolein is directly correlated to the extent of the participation of lattice oxygen.

On the other hand, some rare earth oxides which have nonstoichiometric composition in wide range of oxygen contents, e.g.,  $\text{Pr}_6\text{O}_{11}$  or  $\text{Tb}_4\text{O}_7$ , sometimes showed higher catalytic activity than the other rare earth sesquioxides in the catalytic oxida-

tion, such as oxidation of nitric oxide (3) or oxidation of butane (4). In the previous paper (3), the authors presented that the unstable lattice oxygen of  $\text{Pr}_6\text{O}_{11}$  was desorbed (evolved) by TPD method and showed some lattice oxygen in  $\text{Pr}_6\text{O}_{11}$  to react with nitric oxide to form nitrogen dioxide. Concerning the thermal behavior of the lattice oxygen in the praseodymium oxide, many thermodynamic studies have been made by many authors (5-8); however, kinetic data for the desorption (evolution) of lattice oxygen and absorption of oxygen have scarcely been performed.

In the present study, the thermal behaviors of the lattice oxygen in praseodymium oxide were investigated quantitatively by a TPD technique, X-ray photoelectron spectroscopy (XPS) and X-ray diffractometry, in order to know the catalytic behaviors of lattice oxygen on the oxidation reactions.

### EXPERIMENTAL

*Materials.* The praseodymium oxide (99.9%) was prepared by calcining the oxalate in a stream of an  $\text{O}_2$ - $\text{N}_2$  mixture ( $\text{O}_2$  :  $\text{N}_2$

= 1:4) at 950°C for 6 hr. This oxide was identified as  $\text{Pr}_6\text{O}_{11}$  by X-ray diffractometry. The surface area was 2.3  $\text{m}^2/\text{g}$  by the BET method using nitrogen adsorption at 77 K. The oxygen from a commercial cylinder was purified by bulb-to-bulb distillation with liquid nitrogen coolant. Nitric oxide of a high purity in a glass cylinder from the Takachiho Co. was used without further purification.

**TPD apparatus and the procedure.** The TPD apparatus was a conventional one capable of evacuation to  $10^{-5}$  Torr (1 Torr = 133.3  $\text{N m}^{-2}$ ) by a diffusion pump, and the schematic diagram of it was shown in Fig. 1. The TPD spectra were followed by the variation of pressure with a highly sensitive pirani gauge (Dan Kagaku, Ltd., Model PS-12,  $10^{-4}$  ~ 10 Torr range) due to desorption of the gases from the sample. The usual procedure of TPD was as follows: (1) putting 0.014 g of  $\text{Pr}_6\text{O}_{11}$  in the TPD cell, (2) heating the cell at 750°C for 1 hr in vacuum ( $10^{-5}$  Torr), (3) cooling to a desired temperature, (4) introducing oxygen into the cell, (5) being allowed to stand for the desired time, (6) pumping off the gaseous phase at the same temperature, (7) cooling the cell to 25°C, (8) heating the cell at a rate of 20°C/min in vacuum, and the pressure change due to desorption was recorded. In order to obtain quantitative TPD data, a thermomicrogravimetry was

adopted by using a handmade Gulbransen-type microbalance set in a high vacuum apparatus which is capable of evacuation to  $10^{-5}$  Torr. The XPS spectra were observed with a Vacuum Generator ESCA-3 spectrometer which has a facility of heating the powdered sample *in situ* up to 600°C. The desired  $\text{PrO}_x$  sample was prepared by heating a  $\text{Pr}_6\text{O}_{11}$  in vacuum in the analyzing chamber at various temperatures for 10 min. The source of the X-ray was  $\text{MgK}\alpha$  or  $\text{AlK}\alpha$ . The X-ray diffractometry was carried out with a powder method in atmosphere at room temperature using  $\text{CuK}\alpha$  as an X-ray source (30 kV, 40 mA). The oxygen uptake of the oxide in atmosphere was negligible within 3 hr after the removal of the oxide from the TPD cell. The gas analysis was performed by a mass spectrometer (JEOL, JMS-D-100).

## RESULTS AND DISCUSSION

### 1. TPD Spectra of $\text{PrO}_x\text{-O}_2$ System

Figure 2 shows the TPD spectra obtained from the  $\text{PrO}_x\text{-O}_2$  system for the various oxygen-treatment temperatures [TPD procedure (3) described in the experimental section]. The oxygen pressure and time of absorption were 400 Torr and 1 hr, respectively [TPD procedure (4) and (5)]. The spectrum (a) obtained from the sample oxy-

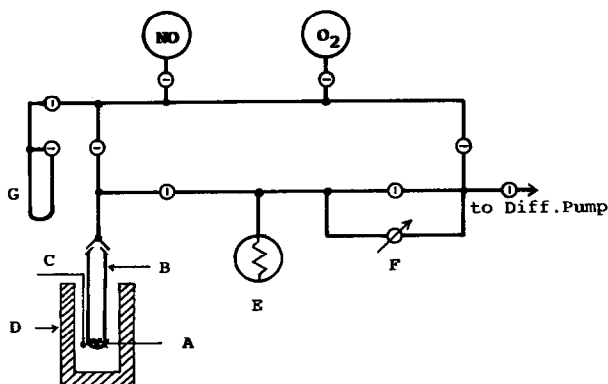


FIG. 1. Block diagram of a TPD apparatus. A, sample; B, TPD cell; C, thermocouple (c.a.); D, furnace; E, pirani gauge; F, variable leak stop-cock; G, manometer (Hg).

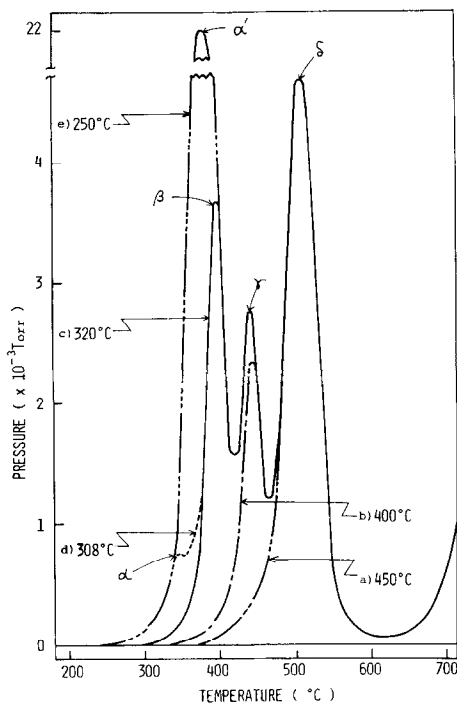


FIG. 2. TPD spectra of the  $\text{PrO}_x\text{-O}_2$  system for various oxygen-treatment at different temperatures. Oxygen-treatment was performed at a pressure of different temperatures: (a) 450°C; (b) 400°C; (c) 320°C; (d) 308°C; (e) 250°C.

gen-treated at 450°C showed only peak  $\delta$  at 500°C. This large peak can be found on all of the sample. The sample oxygen-treated at 400°C gave  $\gamma$  peak at 440°C besides  $\delta$  peak, and that treated at 320°C gave also  $\beta$  peak at 400°C besides  $\gamma$  and  $\delta$  peaks. The samples treated oxygen at 450, 400, and 320°C showed the maximum temperatures, at which the peak heights of each characteristic peaks  $\delta$ ,  $\gamma$ , and  $\beta$  were maximum, respectively. When the sample was treated with oxygen at the temperature between 302 ~ 308°C, a small peak  $\alpha$  also appeared at 340°C; however, when it was treated at less than 300°C a large peak  $\alpha'$  appeared at around 380°C in which both  $\alpha$  and  $\beta$  peaks were also included. At less than 200°C of oxygen-treatment temperature, the intensity of each peak was much weaker than that obtained at higher temperatures of oxygen-treatment as shown in Fig. 2. The

virgin oxide which was not treated by either the evacuation at 750°C or the oxygen absorption at a certain temperature [TPD procedure (2) ~ (7)] gave only  $\beta$ ,  $\gamma$ ,  $\delta$  peaks. The detailed examination on the TPD spectra of  $\alpha$  and  $\alpha'$  peaks will be given in a separate paper. Oxygen desorption occurring from 670°C on every TPD spectra was not considered in the present study, because the oxidation reaction was performed below this temperature. Then, all the desorbed gas followed on the TPD spectra was assigned to oxygen by mass spectrometry.

Figure 3 shows the influence of oxygen-treatment time on the TPD spectra, in which 400 Torr of oxygen was introduced at 320°C for their oxygen-treatments [TPD procedure (4) ~ (6)]. Both oxygen of  $\gamma$  and  $\delta$  were saturated within 3 min. The  $\beta$  oxygen was saturated after about 1 hr; nevertheless about 80% of it was absorbed in 1 min after the introduction of oxygen. The effect of absorption pressure on the TPD

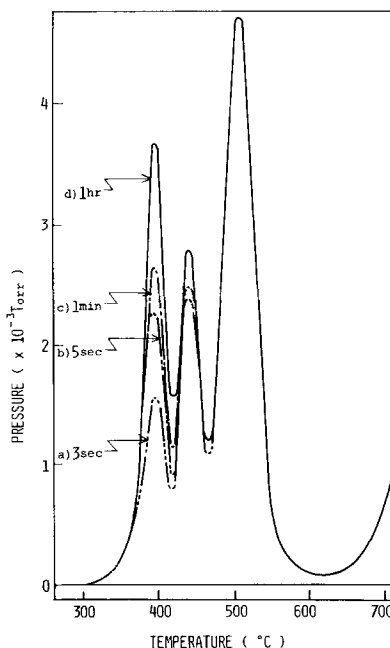


FIG. 3. The time dependence of absorption time of oxygen to 400 Torr of oxygen pressure at 320°C. (a) 3 sec; (b) 5 sec; (c) 1 min; (d) 1 hr.

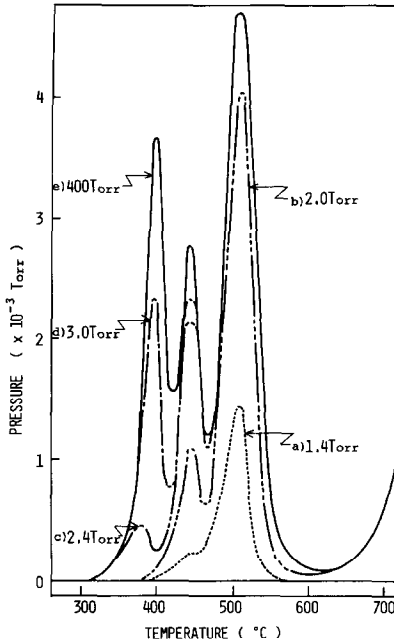


FIG. 4. The pressure dependence of oxygen to the TPD spectra in the  $\text{PrO}_x\text{-O}_2$  system at  $320^\circ\text{C}$  for 1 hr. (a) 1.4 Torr; (b) 2.0 Torr; (c) 2.4 Torr; (d) 3.0 Torr; (e) 400 Torr.

spectra was shown in Fig. 4 in which the sample was treated with oxygen at  $320^\circ\text{C}$  for 1 hr [TPD procedure (4) ~ (6)]. The absorption pressure of oxygen after the oxygen absorption was just the same as that before the evacuation at  $320^\circ\text{C}$  after the oxygen absorption. When absorption pressure was 1.4 Torr, only the  $\delta$  peak accompanied with a small  $\gamma$  peak was observed. The intensities of  $\delta$  and  $\gamma$  peaks rapidly increased with increase of the absorption pressure and were almost saturated at 2.4 Torr, while the intensity of  $\beta$  peak increased rather slowly with the rise in absorption pressure and was saturated at about 10 Torr, as shown in Fig. 5.

From the desorption spectra obtained, the activation energies of the desorption of oxygens assigned to each peak were calculated by the method proposed by Cvetanović and Amenomiya (9). When the temperature of sample linearly increases with time, the peak maximum temperature ( $T_M$ ) of desorption is correlated with the

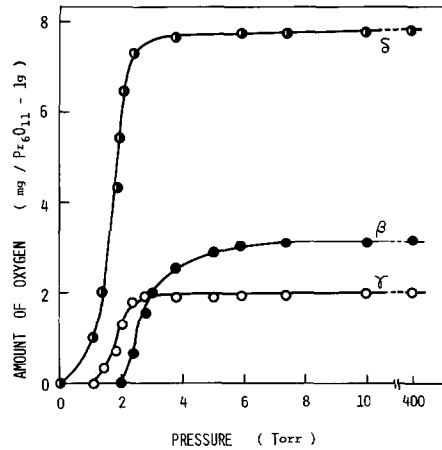


FIG. 5. Relation between the amount of each TPD peak oxygen absorbed in the praseodymium oxide and the oxygen pressure for absorption at  $320^\circ\text{C}$  for 1 hr.

activation energy of desorption ( $E_d$ ) and the heating rate ( $R$ ) by the following equation:

$$2 \ln T_M - \ln R = E_d / RT_M + \ln E_d V_m / R k_0,$$

where  $V_m$  is the amount of oxygen desorbed per unit volume of the solid phase when  $\theta = 1$ ,  $k_0$  is the preexponential factor of the rate constant of desorption. By plotting  $2 \ln T_M - \ln R$  against  $T_M^{-1}$ ,  $E_d$  can be determined. Figure 6 shows this relation for  $\beta$ ,  $\gamma$ ,  $\delta$  peak oxygens. From this figure the activation energies of desorption for the  $\beta$ ,  $\gamma$ , and  $\delta$  peak oxygens were estimated to be 34, 43, and 43 kcal/mol, respectively. The energy

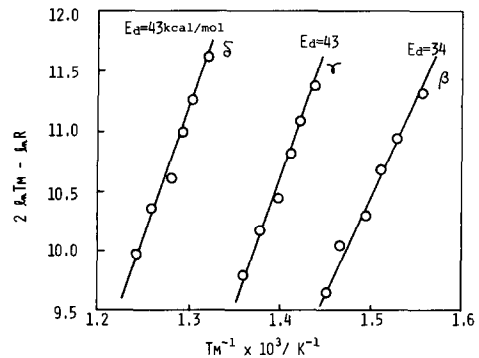


FIG. 6. The plots for the determination of the activation energy of desorption of each TPD peak oxygens in  $\text{Pr}_6\text{O}_{11}$ . Oxygen-treatment at 400 Torr at  $320^\circ\text{C}$  for 1 hr. Rate of temperature increase was changed from 5 to  $30^\circ\text{C}/\text{min}$ .

of desorption for  $\beta$  peak oxygen was lower than those obtained from  $\gamma$  and  $\delta$  peak oxygens. Therefore, we could say that  $\gamma$  and  $\delta$  peak oxygens have quite similar behaviors as to the absorption rate, equilibrium pressure to absorption and desorption processes, whereas the desorption temperature of  $\gamma$  oxygen peak was about 80°C lower than that of  $\delta$  oxygen peak, and the  $\beta$  oxygen peak having slower absorption rate and higher equilibrium pressure of absorption has lower activation energy of desorption than those of  $\gamma$  and  $\delta$  oxygen peaks.

## 2. Structure and Surface Characteristics of PrO<sub>x</sub>

Figure 7 shows X-ray diffraction spectra of PrO<sub>x</sub> which has various TPD oxygen peaks. The lattice constant of the sample for the spectrum (d) was almost identical

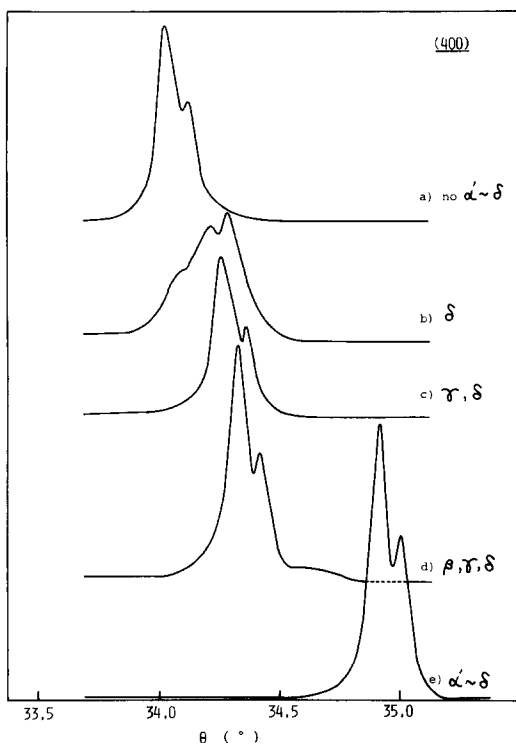


FIG. 7. X-Ray diffraction spectra of PrO<sub>x</sub> with various TPD oxygen peaks. Pretreatment was the same as that described in Fig. 1. X-Ray diffraction was carried out in atmosphere at room temperature.

TABLE 1

The Structure of Praseodymium Oxide Having Various Oxygen Peaks

	Oxygen peaks found in TPD spectrum	Value of $x$ in PrO <sub>x</sub>	
		By X-ray diffractometry	By gravimetry
(a)	No peak	1.68	1.67
(b)	$\delta$	1.78	1.77
(c)	$\gamma, \delta$	1.81	1.79
(d)	$\beta, \gamma, \delta$	1.84	1.83
(e)	$\alpha', \gamma, \delta$	2.0	2.0

to that of Pr<sub>6</sub>O<sub>11</sub> ( $a_{fcc} = 5.4695$ ). The lattice constant was calculated from the diffraction peaks of (400), (331), (420), and (422) planes of the oxide. Therefore, not only the spectral features of TPD but also X-ray diffraction spectra of Pr<sub>6</sub>O<sub>11</sub> were identical with those of the praseodymium oxide which were oxygen-treated in 400 Torr of oxygen at 320°C for 1 hr after the evacuation at 750°C. The value of  $x$  in the formula PrO<sub>x</sub> for the samples with various TPD oxygen peaks are listed in Table 1. The  $x$  value was determined by two methods, i.e., the X-ray diffractometry and the thermogravimetry. In the case of the X-ray diffractometry, the  $x$  value was estimated from the relation between the  $x$  value and the lattice constants of this oxide system (5). The  $x$  value determined by both methods gave almost the same result within experimental errors. According to the phase diagram of praseodymium oxide presented by Burham and Eyring (6), there are six oxides in the range of  $x = 1.5 \sim 2.0$ , i.e., PrO<sub>1.50</sub>, PrO<sub>1.714</sub>, PrO<sub>1.778</sub>, PrO<sub>1.80</sub>, PrO<sub>1.833</sub>, and PrO<sub>2.0</sub> in the temperature range taken in our experimental conditions. The  $x$  values of the latter four oxides were coincided with those of the oxide (b), (c), (d), and (e) shown in the table; however, both the former two oxides do not coincide with the oxide (a). On the other hand, Honig and co-workers (7) studied the value of  $x$  as functions of oxygen pressure and temperature, and obtained eight oxides in the range of  $x$

$= 1.5 \sim 1.833$ , i.e.,  $\text{PrO}_{1.50}$ ,  $\text{PrO}_{1.62}$ ,  $\text{PrO}_{1.67}$ ,  $\text{PrO}_{1.71}$ ,  $\text{PrO}_{1.78}$ ,  $\text{PrO}_{1.80}$ ,  $\text{PrO}_{1.82}$ , and  $\text{PrO}_{1.833}$ . The oxides  $\text{PrO}_{1.67}$ ,  $\text{PrO}_{1.78}$ ,  $\text{PrO}_{1.80}$ , and  $\text{PrO}_{1.833}$  coincide with the oxides listed in the table. Siegraff and Eyring (10) obtained two crystalline oxide phases,  $\text{Pr}_6\text{O}_{11}$  and  $\text{PrO}_2$ , when the oxidized a  $\text{Pr}_6\text{O}_{11}$  sample at  $350^\circ\text{C}$  under oxygen pressure of 4.25 atm. In the present study, the oxide giving a large diffraction intensity due to  $\text{PrO}_{2.0}$  was prepared at  $250^\circ\text{C}$  in 400 Torr of oxygen after the evacuation at  $750^\circ\text{C}$ . The evacuation at a high temperature seems to promote the oxygen-uptake into the lattice, resembling the oxygen-uptake onto NiO by an evacuation treatment at a high temperature reported by Iwamoto and co-workers (11). The close agreement of the value of  $x$  determined from the X-ray diffractometry and the microgravimetry means that most of the desorbed oxygen from the praseodymium oxide by heating *in vacuo* originated from the lattice oxygen of the oxide; however, the oxygen existing on surface layers as lattice oxygen might be more sensitive and removable to the heat treatment to the oxides.

Figure 8 shows the XPS spectra of the

praseodymium oxides with the various oxygen peaks which were heat-treated at various temperatures in the XPS chamber. The spectral features of  $\text{Pr}3d_{5/2}$  from the praseodymium oxide were scarcely affected by the temperature of treatment. On the other hand, the spectral features of  $\text{O}_{1s}$  were strongly affected by these heat treatments. That is, the intensity of peak having the higher binding energy decreased with the increase in the heat-treatment temperature. The ratios of peak intensities at  $\sim 531$  eV to  $\sim 528$  eV of (a), (b), (c), and (d) were 1.1, 0.67, 0.67, and 0.59, respectively. This fact suggests that weakly bounded oxygen, probably the lattice oxygen in the surface layers, was more easily desorbed by the heating than that in the bulk by that treatment, whereas most of the desorbed oxygen came from the bulk, because the total amount due to  $\beta$ ,  $\gamma$ , and  $\delta$  oxygen peaks was at most about 7.5% of oxygen in  $\text{Pr}_6\text{O}_{11}$ .

### 3. Reactivity of the Lattice Oxygen in $\text{Pr}_6\text{O}_{11}\text{NO}$

As already presented qualitatively in the previous paper (3), only the  $\beta$  peak oxygen

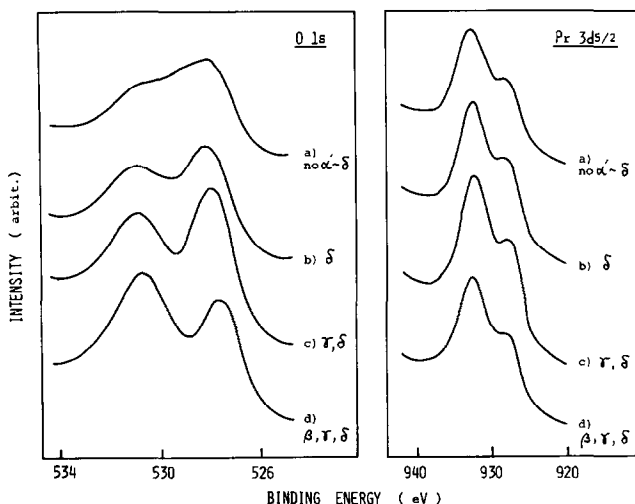


FIG. 8. XPS spectra of  $\text{PrO}_x$  with various TPD oxygen peaks. The samples were prepared by heating a  $\text{Pr}_6\text{O}_{11}$  *in vacuo* in the analyzer chamber at various temperatures: (a)  $600^\circ\text{C}$ ; (b)  $460^\circ\text{C}$ ; (c)  $370^\circ\text{C}$ ; (d)  $290^\circ\text{C}$ .

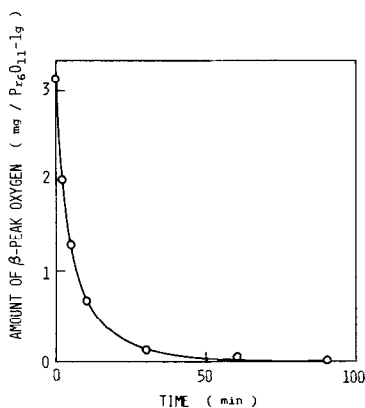


FIG. 9. Consumption of the  $\beta$  oxygen peak in  $\text{Pr}_6\text{O}_{11}$  by NO. Reaction was carried out in 10 Torr of NO at  $280^\circ\text{C}$ .

among  $\beta$ ,  $\gamma$ , and  $\delta$  oxygens could be reacted with NO at around  $300^\circ\text{C}$ . Figure 9 shows the time course of the reaction of  $\beta$  oxygen in  $\text{Pr}_6\text{O}_{11}$  with 10 Torr of NO at  $280^\circ\text{C}$ . In this case, the peak intensities of  $\gamma$  and  $\delta$  in their TPD spectra were not affected during the reaction. In the early stage, the rate of reaction of  $\beta$  oxygen with NO closely obeyed a parabolic rate law  $(\Delta W)^2 = k_p t$ , where  $\Delta W$  signifies the amount of oxygen consumed,  $k_p$  the parabolic rate constant, and  $t$  the reaction time. This fact suggests that the reaction rate should be controlled by the diffusion rate of the lattice oxygen from the bulk to the surface. The apparent activation energy of the reaction was 21 kcal/mol between 200 and  $300^\circ\text{C}$ . The con-

tribution from each oxygen peak, especially the  $\alpha'$  and  $\beta$  oxygen peaks, to the rate of oxidation reactions of NO in detail is now being studied.

#### ACKNOWLEDGMENTS

One of the authors (Y.T.) gratefully acknowledges the support of a part of this research by a grant from Itoh Kagaku Shinkokai. This research was also generously supported in part by the Science Research Grant, No. 34300 I, from the Ministry of Education, Japan and Grant from Mitsubishi Foundation, 1979 (I.T.).

#### REFERENCES

1. Keulks, G. W., *J. Catal.* **19**, 232 (1970).
2. Moro-oka, Y., Ueda, W., Tanaka, S., and Ikawa, T., Proc. 7th Int. Cong. Catal., Tokyo, B-30 (1980).
3. Takasu, Y., Nishibe, S., and Matsuda, Y., *J. Catal.* **49**, 236 (1977).
4. Hattori, T., and Murakami, Y., *Shokubai (Catalyst)* **18**, 41 (1976) (in Japanese).
5. Sawyer, J. O., Hydde, B. G., and Eyring, L., *Bull. Soc. Chim. Fran.* 1190 (1965).
6. Burham, D. A., and Eyring, L., *J. Phys. Chem.* **72**, 4415 (1968).
7. Honig, J. M., Clifford, A. F., and Feath, P. A., *Inorg. Chem.* **2**, 791 (1963).
8. Kunzmann, P., and Eyring, L., *J. Solid State Chem.* **14**, 229 (1975).
9. Cvetanović, R. J., and Amenomiya, Y., in "Advances in Catalysis" (D. D. Eley, H. Pines, and P. B. Weisz, Eds.), Vol. 17, p. 103. Academic Press, New York, 1967.
10. Sieglaff, C. L., and Eyring, L., *J. Amer. Chem. Soc.* **79**, 3024 (1957).
11. Iwamoto, M., Yoda, Y., Egashira, M., and Seiyama, T., *J. Phys. Chem.* **80**, 1989 (1976).